

PRELIMINARY RESULTS FROM FIELD EXPERIMENTAL STUDY OF RAIN LOAD AND PENETRATION INTO WOOD-FRAME WALL SYSTEMS AT WINDOW SILL DEFECTS

E. Ngudjiharto, F. Tariku and P. Fazio

ABSTRACT

A field study is presented here on the investigation of the correlation between wind-driven rain (WDR) as the driving force and the relative proportions of water penetration at intended defects (openings) located at the interface of windows and exterior walls. In this field study, eight full-scale exterior-wall panels of vinyl siding and stucco claddings were built and installed on a field testing station, which is subjected to British Columbia's west coast climate rain. This paper focuses on the preliminary results from one of the stucco wall panels with a discontinuity in the sealant around the perimeters of the windows. The water passing through this defect was collected and measured. The instantaneous and automatic water collection measurements were synchronized to the data gathered by a nearby weather station on wind-driven rain intensity, wind speed and direction. In addition, rain gauges on exterior of walls collected the wind-driven rain against each façade of the test station. Compared to previous computer simulations and laboratory experimental studies on rain penetration through exterior walls, this study was conducted under more realistic conditions. The panels were subjected to real wind-driven rain events. Also collectively, the experiment took into account rain that splashed off the wall façade upon impact and the rain water around the defect location due to run-off. The study is ongoing. However, when complete, the results from this study will be useful for fine-tuning the principal moisture load that is applied in hygrothermal performance assessment and design of exterior wall systems.

INTRODUCTION

Among several sources for exterior moisture ingress at wall details, rainwater penetration is the main source to the majority of the problems found in the 1999 Survey of Building Envelope Failures in the Coastal Climate of British Columbia (Morrison Hershfield Ltd., 1996). In response to these past moisture-related wall failures, the building science industry is gaining interest in predicting the wetting and drying performance of a wall assembly in a particular climate conditions (Tariku et al., 2007). For a systematic building envelope moisture performance evaluation, ASHRAE developed a standard called ASHRAE Standard 160 - Criteria for Moisture Control Design Analysis in Buildings (2009).

The Standard is a guide that helps building designers decide on building envelope assembly designs that are suitable for the building's climate and the potential moisture load on that envelope. Section 4.6 of this ASHRAE Standard addresses the rain penetration as a moisture load source by first calculating the design rain loads on the walls exposed to the rain, and then assuming that a portion of that rain load penetrates the wall as follows.

“In the absence of specific full-scale test methods and data for the as-built exterior wall system being considered, the default value for water penetration through the exterior surface shall be **1% of the water reaching the exterior surface.**” (ANSI/ASHRAE Standard 160, 2009)

However, due to lack of sufficient data, this 1% percentage is arbitrarily determined based on unpublished research on brick walls (TenWolde, 2008). There is a need to investigate in the field the correlation between

the rain penetration and the wind-driven rain parameters. A field experimental study has been conducted at British Columbia Institute of Technology (BCIT) in Burnaby, British Columbia (BC) to fill this research need.

The objective of this study is to find the correlations between measured amounts of rainwater collected through various specified defects to the corresponding rain and wind data recorded during fall and winter rain events in BC. At this time, the scope of the study is limited to defects on vinyl siding and stucco cladded wood frame walls at window sill interface. This paper presents the preliminary findings from one defect type at one of the stucco wall panels during the month of September 2013.

WALL PANELS CONSTRUCTION AND TEST FACILITY

Eight 4ft x 8ft wall panels were constructed, installed onto the ground level of south east façade of BCIT Building Envelope Test Facility (BETF), Burnaby, and cladded with vinyl siding and stucco to the full 16ft height of the façade in the summer of 2013.

The test facility is located in an area surrounded by a parking lot to the west, a grassy area to the north, a small downhill (about 4ft high) area leading to another parking lot to the south, and some trees about 26 feet to the east. The test facility can accommodate up to 16ft high walls and was maintained at 21°C and 50% RH on the interior throughout the year. Test panels were subjected to naturally occurring weather condition from the exterior. A weather station located on BCIT Burnaby campus monitored the weather components, such as rainfall intensity, wind speed and wind direction.

For this study, only the first-storey panels were newly constructed to incorporate the sensors and measuring devices, while the previously framed top-storey walls were preserved or built-up to the same depth and finished with the same cladding as the bottom walls. Each wall panel specimen was isolated from its surrounding panels with XPS rigid insulation.

In September 2013, four tipping-bucket rain gauges with square catchment plates were placed on the brick walls on the north and south ends of the SE façade at approximately 4ft and 12ft heights above the bottom of the wall panels (Figure 1). More rain gauges were later added after this preliminary test in the middle area of the façade, adjacent to the window sills. The wall rain gauges measured the amount of wind-driven rain every minute to the accuracy of 0.038mm/tip. This paper presents the data collected from Wall 6 (W6) panel's left bottom corner leakage collection where 4in length of sealant and backer rod were missing from the jamb (Figure 2). The location of W6 on the SE façade is shown in Figure 1.

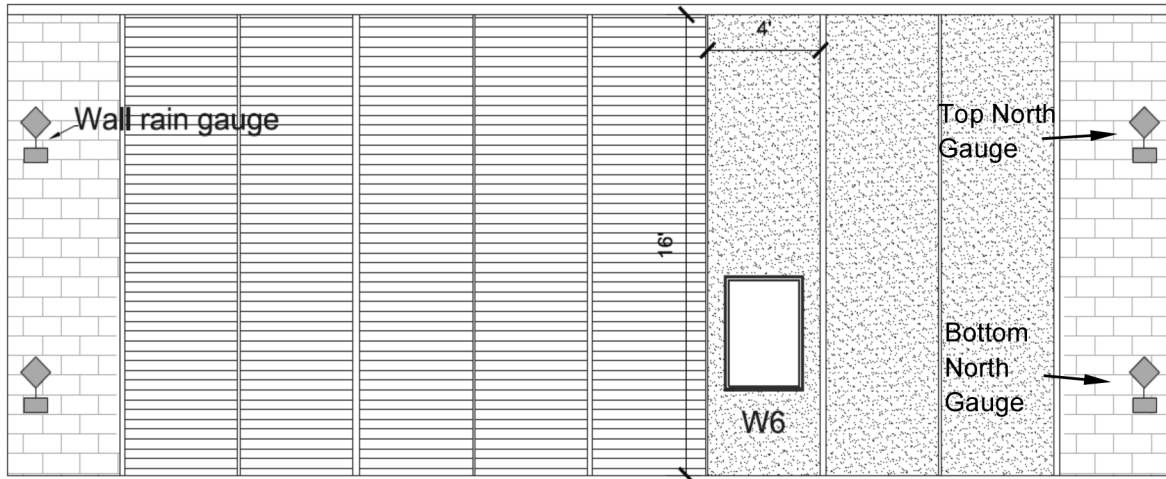


FIGURE 1: SCHEMATIC DRAWING OF WALL 6 (W6) LOCATION ON THE SE FAÇADE AT THE BETF, BCIT, BURNABY, BC.

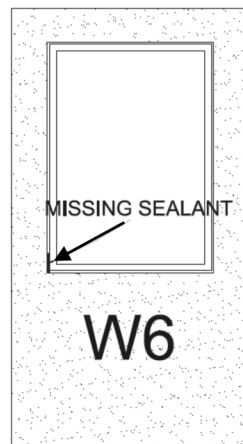


FIGURE 2: LOCATION OF 4IN LENGTH OF MISSING SEALANT AND BACKER ROD AT THE BOTTOM LEFT WINDOW JAMB CORNER OF W6 (ONLY FIRST-STOREY HEIGHT SHOWN).

W6 WALL ASSEMBLY AND INSTRUMENTATION

The wall assembly of W6 was designed to reflect the 1980s housing stock of residential wood-frame construction with stucco cladding, which is still common in British Columbia today. Wood framing was sheathed with plywood, covered with 2 layers of 30-minute building paper, and then cladded with face-sealed stucco on metal lath (Figure 3). The two layers of 30-minute building paper, which are typical of BC area, were used as the water resistive barriers and to promote drainage behind the stucco. While the current British Columbia Building Code does not allow face-seal construction on new construction, many existing residential buildings have this wall type. In the face-seal wall type, any joint details are particularly susceptible to water ingress damage. The bottom corner window sill was therefore chosen as the defect location. The Survey of Building Envelope Failures in the Coastal Climate of British Columbia (Morrison Hershfield Ltd., 1996) found 23% of surveyed building envelope failures occurred at window areas and that missing sealants at the frame/cladding joint was one of the problems observed. The defect at W6 simulated this missing sealant problem at a controlled length of 4 inches up the jamb sealant location.

For this experiment, W6 was modified to collect and measure any rainwater leakage through the defect. As shown in Figure 3, a shelf was framed in the wall cavity of W6 below the sill framing of the defect location to hold a modified tipping bucket rain gauge, which will be referred to as the Leakage Gauge. A trough made from coated, corrosion-resistant aluminum flashing sheet was placed across the plywood sheathing to direct any leakage through the defect onto the tipping bucket counter, which tipped after every 1.618 mL of rainwater was received.

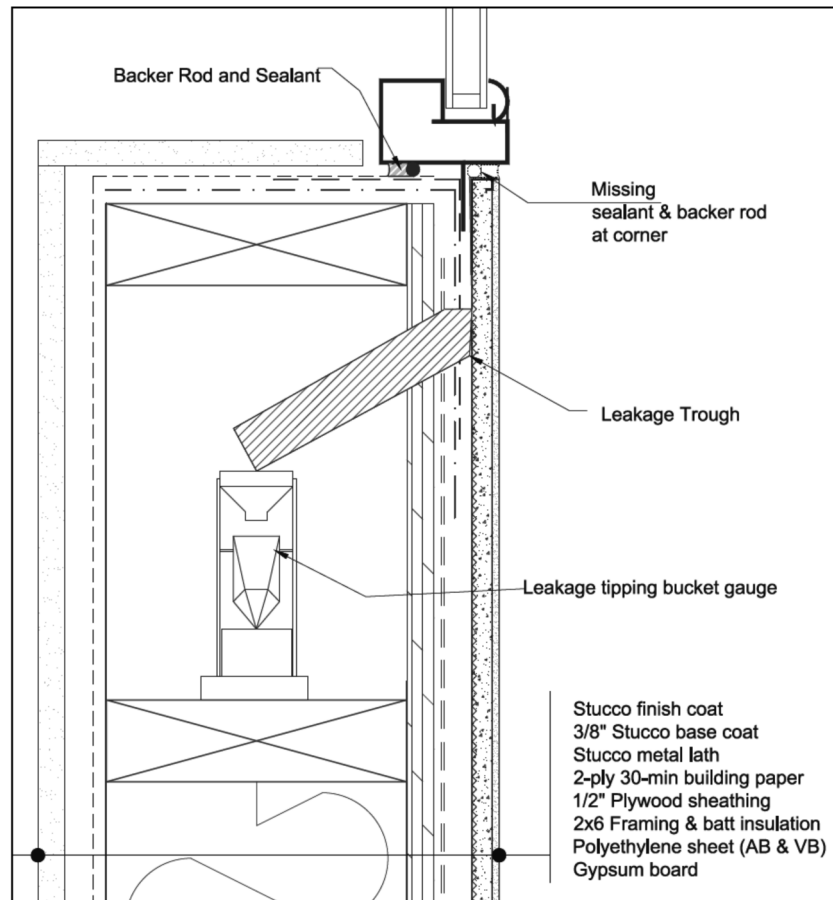


FIGURE 3: WINDOW SILL DETAIL OF W6 STUCCO WALL. ASSEMBLY COMPONENTS WERE TYPICAL FOR ALL STUCCO WALLS IN THIS STUDY; THE LEAKAGE TIPPING BUCKET GAUGE SET UP WAS SPECIFIC FOR W6.

PRELIMINARY RESULTS

RAIN INTENSITY AND WIND CHARACTERISTICS AT TEST LOCATION

Five periods of rain occurred in September 2013. Figure 4 shows the rain loads that the test facility was exposed to. The rain intensity was measured by the horizontal rain gauge on the rooftop of the test facility every minute and then averaged for hourly rate. For the same month, the facility was exposed to the wind loads shown in Figure 5. Minute records of wind speed and direction data were used to generate the wind roses. The left wind rose shows that the wind speed is inversely proportional to the frequency of occurrence, such that wind speed of less than 1 m/s occurred most frequently. Southeast wind was the most prevalent wind direction for all wind speed categories. The right wind rose compares the average wind speeds between

wind occurring only during rain and wind occurring anytime in September 2013 for the test facility. The average speed of winds from NE to SE is steadier at the range of 1.2-1.6 m/s during rain or at around 0.8 m/s in general compared to the speed of wind from other directions. The wind roses confirm that SE façade was the windward-facing wall and that the mean of wind speed during rain was greater than that at any time.

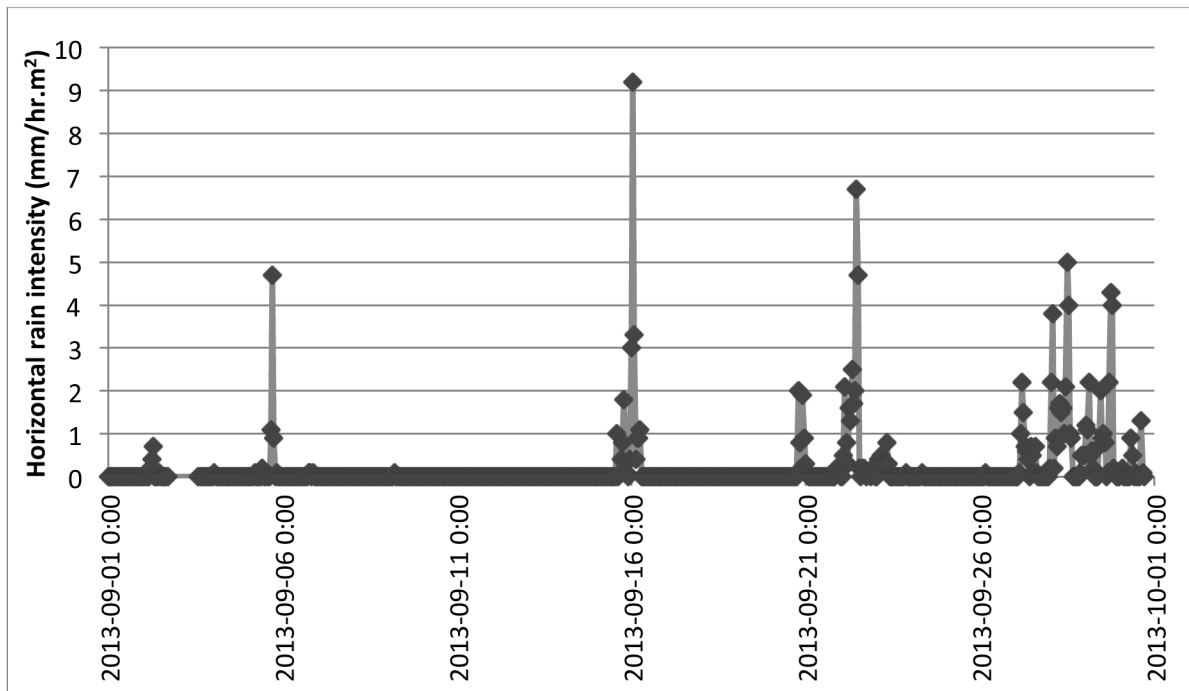


FIGURE 4: HOURLY RAIN INTENSITY MEASURED BY HORIZONTAL RAIN GAUGE ON ROOFTOP OF TEST FACILITY.

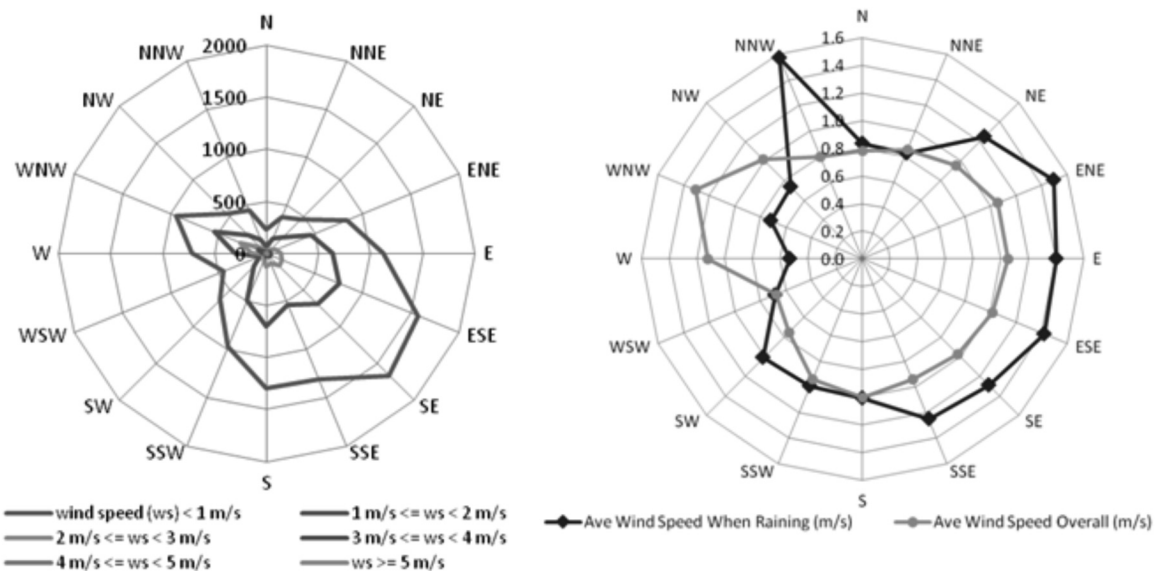


FIGURE 5: FREQUENCY DISTRIBUTION OF MINUTE RECORDS OF WIND DIRECTION AT DIFFERENT WIND SPEEDS (LEFT ROSE) AND DISTRIBUTION AND MAGNITUDES OF AVERAGE WIND SPEEDS WHEN RAINING AND IN GENERAL FOR BCIT BURNABY (RIGHT ROSE) IN SEPTEMBER 2013.

WIND-DRIVEN RAIN ONTO SOUTHEAST FAÇADE OF TEST FACILITY

Compared to the rain intensity measured by the horizontal rain gauge, the range of the hourly rain intensities measured by the two wall gauges on the SE façade, Top and Bottom North gauges, is less than 6% of the range of the hourly rain intensity on horizontal area, as illustrated by Figure 6. While the Bottom North gauge measured all five periods of rain, the Top North gauge did not measure any rain intensities during the first two rain periods on September 2nd and 5th. For these two periods, the Bottom North gauge measured rain intensities of less than 1 mm/hr.m². The bottom north area of SE façade experienced more frequent wind-driven rain at lower magnitude of rain intensity, while the top north area of SE façade was exposed to less frequent wind-driven rain, but at higher intensity. This trend is consistent with the airflow pattern previously found in other research (Blocken and Carmeliet, 2010), where the airflow at the lower area of a wall is complex and the wind speed increases, followed by the wind-driven rain intensity, at upper levels of the wall.

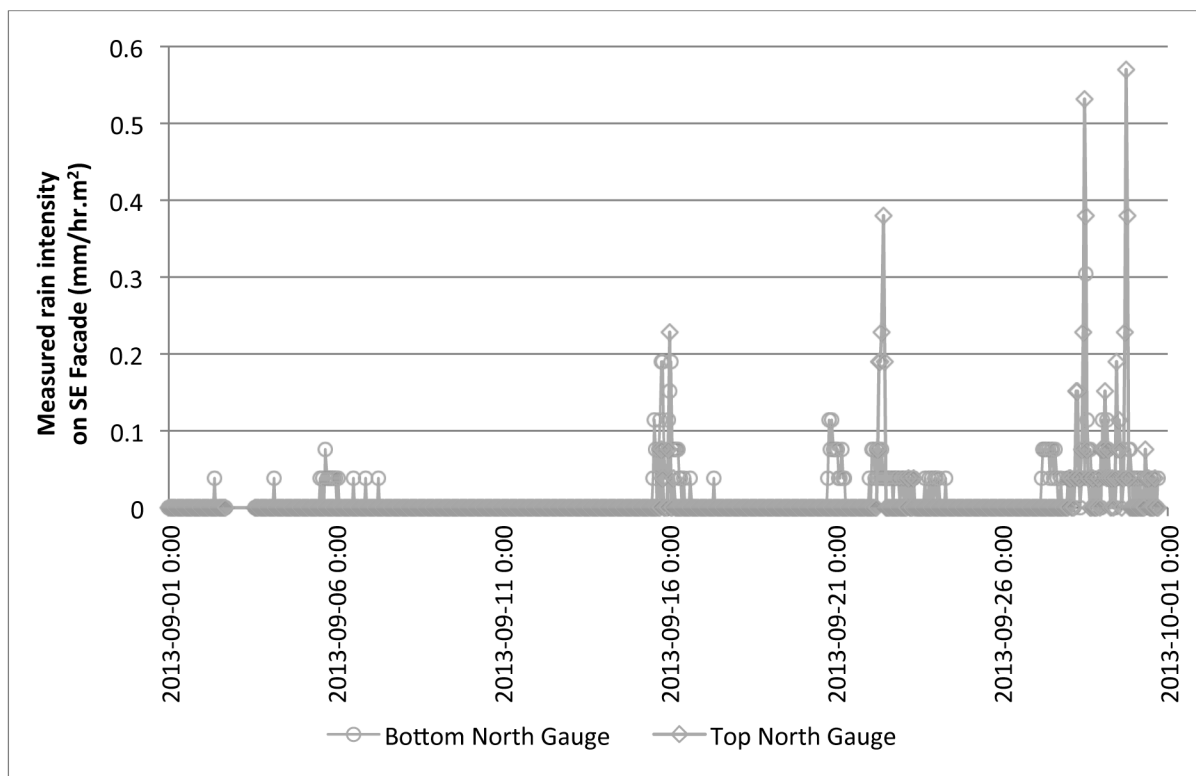


FIGURE 6: MEASURED HOURLY RAIN INTENSITY ON SE FAÇADE NEAR W6 BY TOP AND BOTTOM NORTH GAUGES.

CALCULATED WIND-DRIVEN RAIN

Wind-driven rain that the whole southeast façade was exposed to was calculated following a modified version of the semi-empirical mathematical model by Straube and Burnett (2000). Factors considered in this modified model include the rain intensity measured on horizontal surface, raindrop diameter, wind speed, wind direction, and azimuth angle of the façade of interest. This modified model does not account for the coefficient that factors in the location on the façade, building aspect ratio and presence of overhang, and topography of the building. In essence, without that coefficient, this calculated wind-driven rain is simply the quantity of driving rain that would occur on a vertical surface of 1m² at the height of 10 m (the height of

the wind anemometer on top of the test facility) above ground level in the middle of a free-flowing air field. The calculated wind-driven rain presented in this paper follows the equation below:

$$R_{\text{wdr}} = \text{DRF}(r_h) \cdot \cos(\theta) \cdot V(h) \cdot r_h$$

where R_{wdr} = wind-driven rain on to a vertical surface (mm/hr.m²)

$\text{DRF}(r_h)$ = driving rain factor which depends on the terminal velocity of raindrops,

i.e. $\text{DRF}(r_h) = 1/V_t(d)$

θ = angle of the wind to the wall normal

$V(h)$ = wind speed at the height of interest (m/s)

r_h = horizontal rain intensity (mm/hr.m²)

(Cornick, et al. 2002; Blocken and Carmeliet 2010; Straube and Burnett 2000)

The terminal velocity of raindrops, $V_t(d)$, depends on the raindrop diameter, d , as follows:

$$V_t(d) = -0.166033 + 4.91844d - 0.888016d^2 + 0.054888d^3$$

The raindrop diameter in Straube's model is the median diameter of raindrops distribution, which is defined such that 50% of raindrops in the air are of a diameter less than this median diameter. The following equation is derived from the raindrop sizes distribution given by Best (1950):

$$D_{50} = 1.30 r_h^{0.232} * 0.69^{1/n}$$

where D_{50} = median diameter (mm)

r_h = horizontal rain intensity (mm/hr)

$n = 2.25$

(Cornick et al., 2002; Blocken and Carmeliet, 2010)

Using the above equations, the calculated hourly wind-driven rain intensities (WDR) that a SE-facing surface area in a free-flowing air field at this test facility location in September 2013 were plotted against the actual hourly WDR intensities experienced and measured by the Top North wall gauge (Figure 7) and by the Bottom North wall gauge (Figure 8).

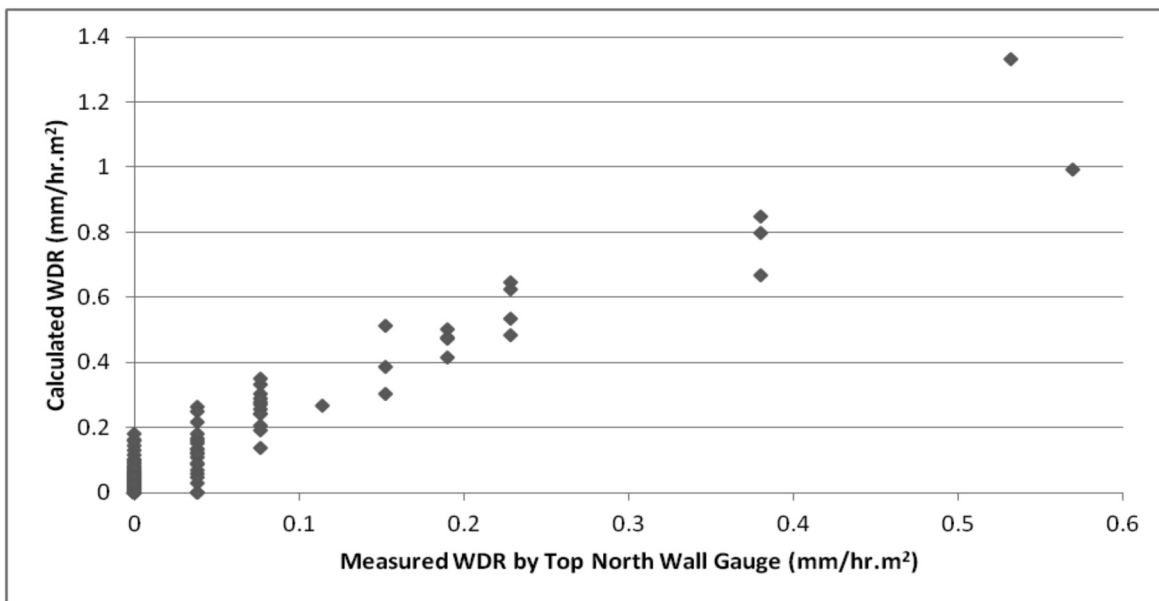


FIGURE 7: CALCULATED HOURLY WIND-DRIVEN RAIN INTENSITY PLOTTED AGAINST MEASURED HOURLY RAIN INTENSITY ON SE FAÇADE NEAR W6 BY TOP NORTH GAUGE.

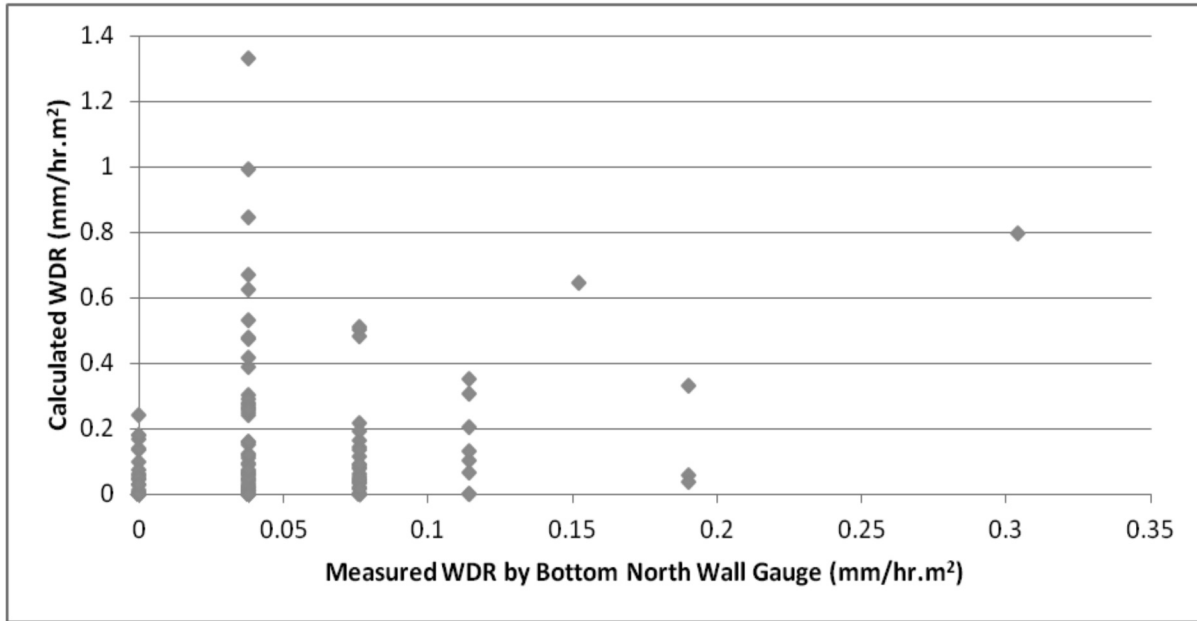


FIGURE 8: CALCULATED HOURLY WIND-DRIVEN RAIN INTENSITY PLOTTED AGAINST MEASURED HOURLY RAIN INTENSITY ON SE FAÇADE NEAR W6 BY BOTTOM NORTH GAUGE.

The trends in Figure 7 and 8 indicate that the correlation between the calculated WDR and Top North wall gauges measured WDR is more pronounced than that of the Bottom North wall gauge. This observation is likely related to the more complex airflow at the bottom wall area, as previously discussed.

Investigating the correlation that is observed between the calculated WDR to the measured WDR by Top North wall gauge is one of the goals of this study. More rain gauges in the middle area of the SE façade were installed after September 2013 and the data analysis and results from these gauges will be presented in future papers.

LEAKAGE AMOUNT AT W6 DEFECT

The above calculated WDR intensities were then plotted against time and compared to the measured leakage amount at W6 corner defect by the Leakage Gauge. As illustrated in Figure 9, this plot shows that the correlation between the calculated WDR intensities and the leakage amount exists. Figure 9 also shows that the early September 5th rain period did not result in any leakage, which is consistent with the low WDR intensities during that period of rain.

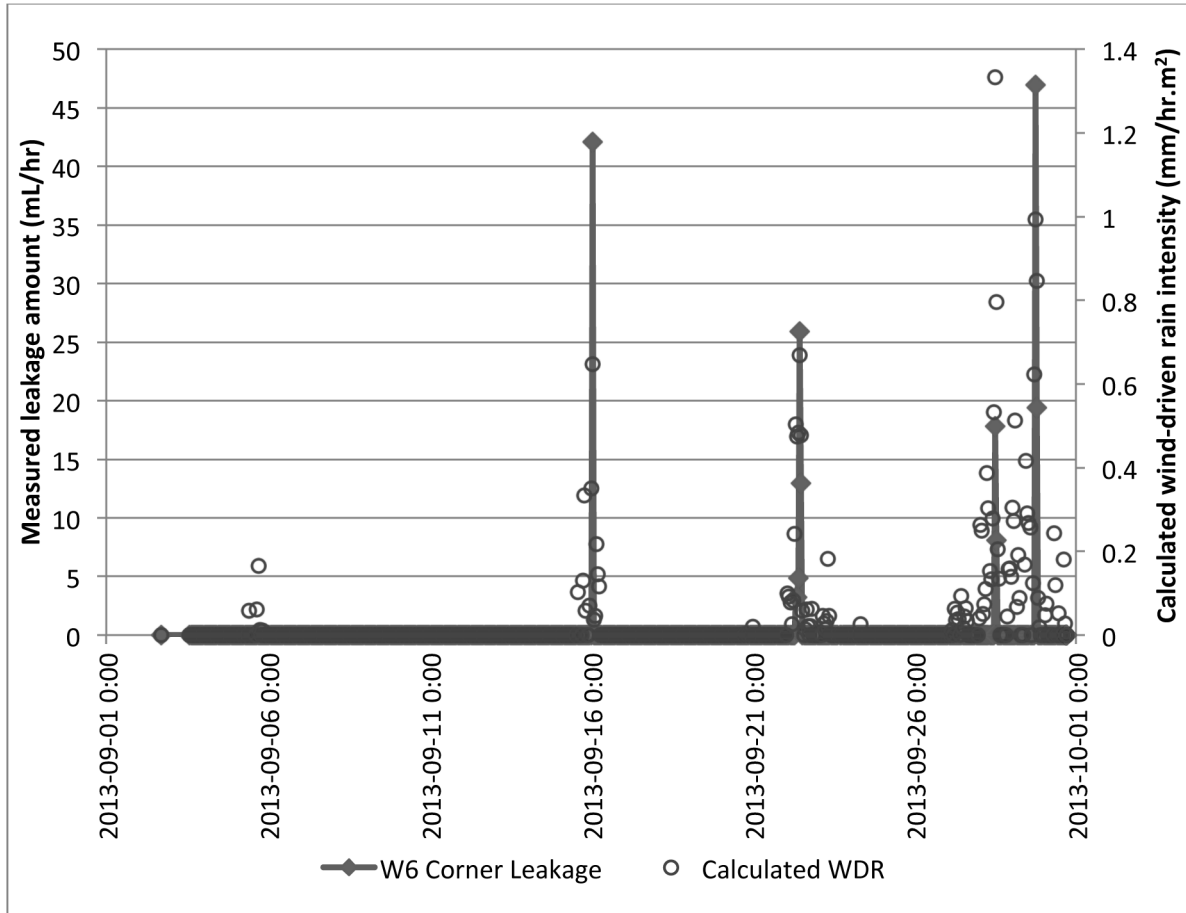


FIGURE 9: COMPARISON OF THE OCCURRENCE AND INTENSITY OF THE CALCULATED WIND-DRIVEN RAIN ON SE FAÇADE TO THE MEASURED LEAKAGE AMOUNT THROUGH CORNER DEFECT OF W6 BY LEAKAGE GAUGE.

CONCLUSION

These preliminary results indicate that there are more factors that need to be considered to estimate the amount of wind-driven rain penetration through walls. However, the discussed results show indications of correlations that could be explored further to arrive at a better prediction of rain penetration through wall defects, such as the one that the ASHRAE Standard 160 aims to achieve. This article only discusses the preliminary results from a small part of this field experimental study. More details and results from a larger data sample of this study will be published in the future.

ACKNOWLEDGEMENT

This study is conducted with the support from British Columbia Institute of Technology (BCIT) in Burnaby, Concordia University in Montréal, and NSERC Canada. The authors wish to thank Doug Horn, Wendy Simpson, Tim Lee and Jordan Ho of BCIT for their assistance in technical and construction aspects of this study.

REFERENCES

- ANSI/ASHRAE Standard 160. 2009. Criteria for moisture-control design analysis in buildings. American Society of Heating, Refrigerating and Air-Conditioning Engineers, Inc., Atlanta, GA.*
- Best, A.C. 1950. The size distribution of raindrops. Quarterly Journal of the Royal Meteorological Society, 76: 16-36.*
- Blocken, B., and Carmeliet, J. 2010. Overview of three state-of-the-art wind-driven rain assessment models and comparison based on model theory. Building and Environment, 45 (3): 691-703.*
- Morrison Hershfield Ltd. 1996. Survey of building envelope failures in the coastal climate of British Columbia. Report for Canada Mortgage and Housing Corporation, Ottawa, Ontario.*
- Straube, J.F. and Burnett, E.F.P. 2000. Simplified prediction of driving rain deposition. Proceedings of International Building Physics Conference, Eindhoven, September 18-21, pp. 375-382.*
- Tariku, F., Cornick, S.M., and Lacasse, M.A. 2007. Simulation of wind-driven rain effects on the performance of a stucco-clad wall. Proceedings of Thermal Performance of Exterior Envelopes of Whole Buildings X International Conference, Clearwater Beach, Florida, December 02, pp. 1-15.*
- TenWolde, A. 2008. ASHRAE Standard 160 P-Criteria for Moisture Control Design Analysis in Buildings. ASHRAE Transactions, 167-171.*